

Vectorial mode characterization of microstructured optical fibers

R. Kotynski, T. Nasilowski and H. Thienpont

Vrije Universiteit Brussels, Department of Applied Physics and Photonics
Pleinlaan 2, B-1050 Brussels, Belgium

We investigate the mode structure and dispersion properties of air-silica microstructured fibers using a fully vectorial numerical model. The transverse electric and magnetic modal fields are expressed as linear combinations of plane-wave type exponential functions. The same basis functions are used to approximate the refractive index of the cross section of the fiber. For fiber profiles composed of cylindrical or elliptical subregions with a constant refractive index (rods, holes, capillars etc.) the Fourier expansion coefficients are found analytically. Boundary conditions are included in the supercell approximation, and finally the model leads to an algebraic eigenproblem which is solved numerically.

Introduction

Accurate modeling of light propagation in micro-structured fibers is highly relevant for tailoring the dispersion, mode area, number of modes and other properties interesting from the point of view of research and at the same time important for the manufacturing process and practical applications. The high refractive index contrasts and fine details with sizes in the order of a wavelength, which are present in the microstructured fiber cross-profiles put special demands on modeling and in particular requires the use of the vectorial description of modes. This implies solving Maxwell's equations with no additional approximations, instead of the scalar or semi-vectorial wave equations, which are accurate enough for common fibers. The approach presented in this paper is a frequency-domain method (as opposed to time-domain methods e.g. related to FDTD), and is based on solving numerically the eigenequation for the transverse field components and the propagation constant in a truncated orthonormal basis.

Model Formulation

In a z-invariant medium, such as an optical fiber, the modes are fully described by the transverse electric or magnetic field distributions \mathbf{e}_\perp and \mathbf{h}_\perp and the propagation constant β . From the Bloch's theorem, one has the following expressions for the modes:

$$\mathbf{E}(\mathbf{r}, t) = \mathbf{e}(\mathbf{r}_\perp) e^{i\beta z} = [\mathbf{e}_\perp(\mathbf{r}_\perp) + e_z(\mathbf{r}_\perp) \hat{\mathbf{z}}] e^{i\beta z}$$

$$\mathbf{H}(\mathbf{r}, t) = \mathbf{h}(\mathbf{r}_\perp) e^{i\beta z} = [\mathbf{h}_\perp(\mathbf{r}_\perp) + h_z(\mathbf{r}_\perp) \hat{\mathbf{z}}] e^{i\beta z}$$

Where, the transverse part of fields satisfies the following eigenequations [1]:

$$[\nabla_\perp^2 + k^2 n^2 - \beta^2] \mathbf{e}_\perp = -[\nabla_\perp \cdot ((\nabla_\perp \ln n^2) \cdot \mathbf{e}_\perp)]$$

$$[\nabla_\perp^2 + k^2 n^2 - \beta^2] \mathbf{h}_\perp = -[(\nabla_\perp \ln n^2) \times (\nabla_\perp \times \mathbf{h}_\perp)]$$

Each of the above two equations is derived directly from Maxwell's equations for a linear and isotropic medium and allows for a fully vectorial description of the electromagnetic modes in a fiber, or any other z-invariant medium. Solving of the modes represents a two-dimensional problem, and the two polarization components of the transverse fields in each of the equations are coupled. Neglecting the coupling

terms, or the entire right-hand side terms leads to semivectorial and scalar approximations respectively, however here we follow the strict vectorial approach. Otherwise, it would indeed be questionable whether the method would be accurate for fiber profiles with a subwavelength microstructure.

At this point we introduce the supercell approximation, i.e. we assume the fields and the cross-profile of the structure to be periodic in the transverse plane. Let \mathbf{a}_1 and \mathbf{a}_2 be the transverse vectors that span the supercell (see Fig. 1). Let S denote the area of the supercell.

We will operate in the reciprocal lattice, spanned with the \mathbf{k} -vectors satisfying the relation:

$$\mathbf{k}_{(n_1, n_2)} \mathbf{a}_1 = 2\pi n_1 \quad \mathbf{k}_{(n_1, n_2)} \mathbf{a}_2 = 2\pi n_2$$

In order to solve the continuous eigenequations numerically, we need to rewrite them in the form of a discrete matrix eigenequation. For that purpose, we go to the following exponential functions basis set:

$$\psi_{\mathbf{n}}(\mathbf{r}_{\perp}) \equiv \psi_{(n_1, n_2)}(\mathbf{r}_{\perp}) = S^{-1/2} \exp(j \cdot \mathbf{k}_{(n_1, n_2)} \cdot \mathbf{r}_{\perp})$$

With $\mathbf{n} \equiv (n_1, n_2) \in Z^2$, our trial functions form a complete orthonormal basis over the supercell, and they satisfy the periodic boundary conditions related to the supercell approximation. It should be emphasized that although we use the basis functions of plane-wave type, the method referred in literature as the plane-wave method is based on a different eigenequation [2].

Obviously, the numerical approach requires truncating the basis set. Also the finite dimension of the supercell is by itself an approximation. The significance of the two approximations depends on computing resources, and sets a trade-off between accuracy, computation speed and memory requirements. In that sense the approximations included in the model, are more of a technical than of a fundamental nature, conversely to the approaches based on solving scalar or semivectorial wave equations.

Before we calculate the matrix elements, we also express the dielectric constant and its logarithm with the use of the same basis functions:

$$\begin{aligned} n^2(\mathbf{r}_{\perp}) &= S^{1/2} \sum_{\mathbf{m}} \varepsilon_{\mathbf{m}} \psi_{\mathbf{m}}(\mathbf{r}_{\perp}) & \varepsilon_{\mathbf{m}} &= S^{-1/2} \langle \psi_{\mathbf{m}} | n^2 \rangle \\ \ln n^2(\mathbf{r}_{\perp}) &= S^{1/2} \sum_{\mathbf{m}} \kappa_{\mathbf{m}} \psi_{\mathbf{m}}(\mathbf{r}_{\perp}) & \kappa_{\mathbf{m}} &= S^{-1/2} \langle \psi_{\mathbf{m}} | \ln n^2 \rangle \end{aligned}$$

One may recognize, that the expansion coefficients ε and κ are determined from the Fourier transform of the cross profile of the refractive index square or logarithm. The purpose of this expansion is to obtain analytical expressions for the matrix elements in the final matrix eigenvalue problem that will be solved numerically. For structures composed of simple-shaped areas with a constant refractive index, such as circular, elliptical or rectangular-shaped areas, coefficients ε and κ may be easily determined analytically, which we actually do here. In that case i.e. for any type of non-gradient fiber, including step-index, multicore fibers, Bragg fibers or holey fibers, the matrix elements can be fully calculated analytically.

We end-up with the following matrix eigenequations for the modes:

$$\left(\begin{bmatrix} \mathbf{Q} & 0 \\ 0 & \mathbf{Q} \end{bmatrix} + \begin{bmatrix} \mathbf{L}_{xx} & \mathbf{L}_{xy} \\ \mathbf{L}_{yx} & \mathbf{L}_{yy} \end{bmatrix} \right) \cdot \begin{bmatrix} \mathbf{h}_x \\ \mathbf{h}_y \end{bmatrix} = \beta^2 \begin{bmatrix} \mathbf{h}_x \\ \mathbf{h}_y \end{bmatrix}$$

$$\left(\begin{bmatrix} \mathbf{Q} & 0 \\ 0 & \mathbf{Q} \end{bmatrix} + \begin{bmatrix} \mathbf{L}_{yy}^+ & \mathbf{L}_{xy}^+ \\ \mathbf{L}_{yx}^+ & \mathbf{L}_{xx}^+ \end{bmatrix} \right) \cdot \begin{bmatrix} \mathbf{e}_x \\ \mathbf{e}_y \end{bmatrix} = \beta^2 \begin{bmatrix} \mathbf{e}_x \\ \mathbf{e}_y \end{bmatrix}$$

$$[\mathbf{Q}]_{n,m} = k^2 \varepsilon_{n-m} - \mathbf{k}_n^2 \delta_{n-m}$$

$$[\mathbf{L}_{xx}]_{n,m} = +k_{ym} k_{y(n-m)} \kappa_{n-m} \quad [\mathbf{L}_{xy}]_{n,m} = -k_{xm} k_{y(n-m)} \kappa_{n-m}$$

$$[\mathbf{L}_{yx}]_{n,m} = -k_{ym} k_{x(n-m)} \kappa_{n-m} \quad [\mathbf{L}_{yy}]_{n,m} = +k_{xm} k_{x(n-m)} \kappa_{n-m}$$

We note that the eigenequation for the magnetic field is generic, while in the equation for the electric field we additionally assumed that the refractive index is real, i.e. there is no absorption. The hermitian symmetry of ε and κ for this case manifests itself beautifully in the similar form of equations for the magnetic and electric fields, even though the original equations from which we started were quite different from each other.

Obviously the last element of the method is the reconstruction of the transverse modal fields from the eigenvectors $\mathbf{h}_x, \mathbf{h}_y$ or $\mathbf{e}_x, \mathbf{e}_y$:

$$\mathbf{h}_\perp = \sum_n (h_{xn} \hat{\mathbf{x}} + h_{yn} \hat{\mathbf{y}}) \nu_n \quad \mathbf{e}_\perp = \sum_n (e_{xn} \hat{\mathbf{x}} + e_{yn} \hat{\mathbf{y}}) \nu_n$$

It is afterwards straightforward to calculate the mode intensity distribution, effective index, birefringence, or group velocity dispersion, although for the dispersion, the result is extremely sensitive to numerical errors. It is also easy to include material dispersion into the model, and for holey fibers we use for this purpose the Sellmeier formula for fused silica.

Since the truncated orthonormal basis methods are widely used for solving eigenequations numerically, we have to acknowledge that similar approaches were already used in the context of holey fibers, however in the authors' opinion, the later still leave important issues. For instance reference [3] seems to finish with a similar, however not exactly equivalent formula (Eq. 6 in [3]). On the other hand, the difficult to follow biorthonormal approach [4] begins with eigenequations (Eq. 2 in [4]) that do not include second order derivatives of the refractive index in the case of electric field, which should at least be commented. Therefore we prefer to present the method in an independent and a self-contained approach.

Mode characterization

In this section we apply our model to solve the modes in an air-silica holey fiber. The fiber that we characterize in this section has a high-silica core, hole diameters equal to $d=1.9\mu\text{m}$ and the lattice constant equal to $\Lambda=5.2\mu\text{m}$.

In order to illustrate our method we plot in Figure 2, as an example, the vectorial mode profile, including electric and magnetic fields and the intensity distribution, calculated at $\lambda=1.55\mu\text{m}$. The presented method allows determining all the basic characteristics of microstructured fibers including those, related to the polarization properties. For instance in Figure 3 we present the wavelength dependence of mode indices, dispersion and birefringence. It is clear that the investigated fiber is single mode for all wavelengths.

As opposed to the scalar methods, our approach allows to study the polarization characteristics of microstructured fibers. Although the structure is not strongly birefringent, we can still show the difference between the two polarization modes making of (Fig. 3c) the fundamental mode.

In the near future we plan to apply this method in the context of dispersion compensated fibers, polarizing fibers and Bragg fibers.

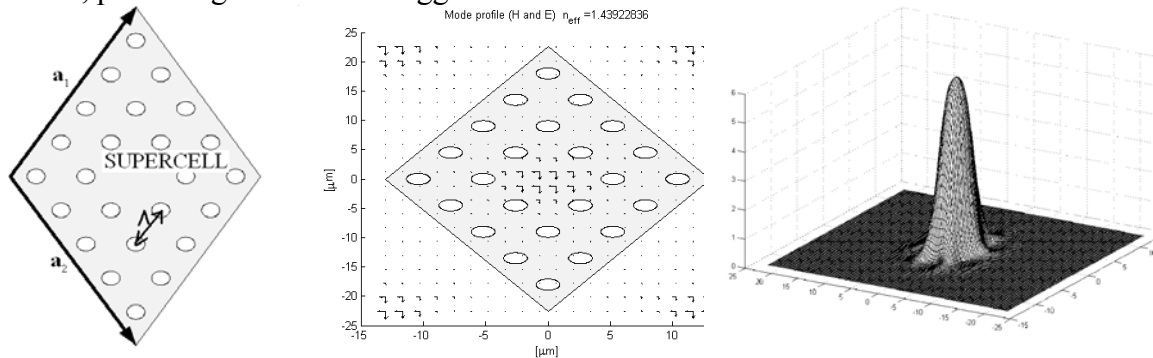


Figure 1: Supercell profile for a typical holey fiber.

Figure 2: Mode profile of the fundamental mode in a holey fiber with $\Lambda=5.2\mu\text{m}$, $d=1.9\mu\text{m}$, $\lambda=1.55\mu\text{m}$. Electric and magnetic fields (left), and intensity (right).

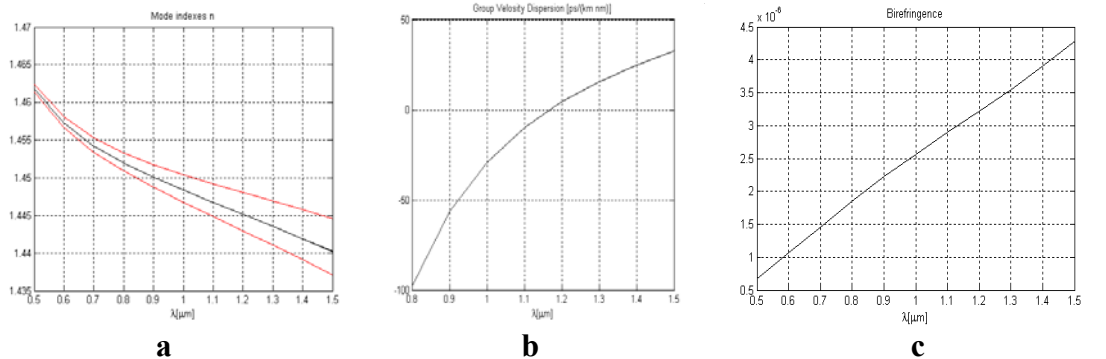


Figure 3. a) Effective refractive index of the fundamental mode (middle), effective index of the cladding (bottom), refractive index of fused silica (top); **b)** Group velocity dispersion **c)** Birefringence

Acknowledgement

We would like to specially thank Krassimir Panajotov for his valuable comments and interesting discussions we had in the context of this work. This work was funded by the FWO, GOA, DWTC IAP Photon Network and the OZR of the Vrije Universiteit Brussel.

References

- [1] A.W. Snyder and J.D. Love Roberts, Optical Waveguide Theory, London and New York, Chapman and Hall, 1983, ch. 30
- [2] S.G. Johnson and J.D. Joannopoulos, "Block-iterative frequency-domain methods for Maxwell's equations in a planewave basis," Opt. Express vol. 8, pp. 173-190,2001
- [3] Z. Zhu and T.G. Brown, "Analysis of the space filling modes of photonic crystal fibers", Opt.Express, vol 8, 2001, pp. 547-554
- [4] A. Ferrando, E. Silvestre, J.J. Miret, P. Andres and M.V. Andres., "Vector description of higher-order modes in photonic crystal fibers", J.O.S.A. vol 7, 2000, pp. 1333-1340.